NOVEMBER 29, 2018

RESILIENCE OF HIGH-STRENGTH STEEL WIDE FLANGE BEAMS TO CORROSION IN SOLAR GROUND MOUNT SYSTEMS

FINAL v.6

JOHN WILLIAMSON P.E., EHTESHAM TARIQ,
THOMAS E. RUSSELL
KILONEWTON LLC
2948 Hyder Ave SE, Albuquerque, NM 87106 USA
1(505)312-8490 www.kilonewtonllc.com

REPORT BACKGROUND

Embedded steel W6 I-beams have historically been one of the most durable and cost-effective materials used in the erection of solar farm foundations. However, the continued need to reduce the installed cost for solar farms has inspired the invention of an even lower cost, yet more durable alternative. W6 I-beams used for guardrail posts and solar foundations are currently produced in grade 50, or 50 ksi. Engineers routinely add sacrificial steel to their foundation designs to account for any potential corrosive loss even if the beam has been hot dip galvanized per ASTM A123 [1]. In areas deemed to have extremely corrosive soils even more sacrificial steel is added to counter corrosive losses. Thomas Russell, industry veteran and steel specialist reasoned that if a steel grade higher than 50 ksi was used, the benefits would be severalfold. Increased bending strength meant greater capacity. This in turn could either allow for a reduction in the designed W6 section size, or if the section size remained consistent with a grade 50 design, then an increase in durability was possible. By utilizing a grade 80, steel material in the production of W6 I-beams he reasoned that the 60% increase in yield strength could be split to reduce the designed grade 50 section size by 30% and, additionally, increase the durability by approximately the same factor.

John Williamson and KiloNewton were contracted by solar steel manufacturer, Attala Steel Industries and Thomas E. Russell, Applicant and Inventor, to conduct an independent study of the technology developed by Russell and which several domestic and international patents were applied for and are currently pending with the US Patent and Trademark Office, USPTO and PCT.

Attala Steel Industries has contracted with the inventor, patent applicant and owner, as the Exclusive North American Licensee to produce and supply the following technology. No other steel supplier, producer or distributor has been authorized to supply without written consent from Attala Steel Industries, Exclusive Licensee for the United States, Canada and the Republic of Mexico.

EXECUTIVE SUMMARY

In this study, W6 wide flange beams (6" I-beams) were analyzed for bending strength under installed conditions with corrosive soils. In typical solar installations, foundations are expected to survive a minimum of 25-30 years. Foundation engineers routinely assume some loss of material due to corrosion over the installed lifetime, which reduces the strength of the material. Hot-rolled steel for I-beams in this size today has 50 ksi yield strength, which is the industry standard. The metallurgy for various higher strength materials had been known, and utilized for different applications, but not for W6 I-beams.

The possibility of producing this higher strength material for W6 I-beams would allow for increasing bending strength but come at a price premium over standard 50 ksi material. In this study, the increase in strength vs. cost efficiency of 65 and 80 ksi materials are analyzed for use in solar foundation applications.

Standard sections and calculation methods were used according to the American Institute of Steel Construction [2], [3] to estimate the capacities of the beams. Though the material strengths increase by 30% and 60% for 65 ksi and 80 ksi material respectively, due to buckling factors, the capacities do not linearly increase with the yield strength. On average, after 30 years in standard corrosion conditions, the same beam size's strength is higher by 26% and 51% compared to the 50 ksi material.

This strength increase allows one to specify lighter foundations in these conditions or have increased safety factors in foundation designs. This study showed that for virtually any situation using heavier I-beam sections, there is a significant cost advantage to using higher strength material instead. Where applicable, a 10-foot high-strength foundation's cost savings potential ranges between $2,000-$10,000/MW, depending on the sizes and quantities of the foundations required on a site. In addition, there are other cost reduction potentials in shipping, and onsite logistics using lighter materials. The potential cost savings increases to scale with longer piles.

INTRODUCTION AND SCOPE

Wide flange beams (or I-beams) have become a standard type of foundation used for most large-scale solar ground-mount photovoltaic projects over the last ten years. W6 sizes are commonly used in the guard-rail industry, which has similar loading, environmental, and lifetime requirements to solar installations. However, the increased popularity of solar utility ground-mount systems has driven new innovations in a relatively old industry, both in the use of uncommon and new sizes, materials and coatings.

I-beams are well suited to the solar ground mount application. Since most of the controlling forces required for solar foundation designs are in a single direction, perpendicular to the plane of the array, I-beams are well-suited due to their material efficiency in resisting bending in a single axis. They also have great skin-friction properties, utilizing all sides of the material. However, corrosion can cause significant reductions in I-beam capacity. Since all sides of the shape are exposed to the elements, corrosion can attack the material more aggressively than closed shapes, such as rounds or squares. They are also more prone to damage during pile driving, particularly in the lighter varieties.

These issues are mitigated by increasing the material yield strength of the beam. In terms of the utility of the beam per pound, virtually every aspect of the beam design is benefitted by increased material

strength. However, higher strength materials come at a higher price as well. Therefore, the costs of the more efficient high strength I-beams must be compared to those of the equivalent lower strength I-beam designs to choose the most cost-efficient option.

KiloNewton was contracted as an independent engineer by, Attala Steel Industries, the exclusive licensee for North America and Thomas E. Russell, inventor of the patent pending technology, to analyze the potential benefits of using higher strength materials for I-beam design in solar applications and prepare this report.

Attala and Russell provided input for the steel shapes and cost estimates for the raw material, however the structural and foundation cost analysis was done completely independently by KiloNewton, using industry standard design principles.

METHODOLOGY

Standard I-beam sections were used for the analysis, according to the AISC Steel Construction Manual [2], along with other less common lightweight sections that are commonly used by the solar industry. The section properties and resulting values for bending strength are calculated for these shapes and correlated to the section property tables in the AISC manual for accuracy.

The section properties were used to calculate the bending capacities using a typical design for a generic solar wide-flange foundation, which is necessary to define for the buckling reduction calculations.

Since soil chemistry can vary greatly, KiloNewton used a simplified approach for estimating corrosion rates. The U.S. Department of Transportation Federal Highway Administration commissioned a report to be published for the American Association of State Highway and Transportation Officials (AASHTO) standards, including corrosion rates to be used in soil fills, along with limits on the soils electrochemical properties [4]. These corrosion rates are considered reasonable for moderately corrosivity soils, so more aggressive corrosion cases were also considered, for which the corrosion rates were multiplied by 2x and 3x for comparison.

The subsequent section properties of the shapes, post-corrosion, were then recalculated according to the *Specification for Structural Steel Buildings* [3], assuming the steel corroded equally over all the surfaces of the I-beams. These new properties were used to estimate the bending strength again for comparison purposes.

Three different material strengths were considered for the study: 50 ksi (considered to be standard in the solar industry), 65 ksi, and 80 ksi. General costs of the foundation material were obtained from Attala Steel, to be used for the purposes of this study. They were given in terms of $/lb, with different costs for each material considered. These unit weight costs were then applied to the shapes to show the most cost-efficient designs for a given bending requirement. These are then presented in the form of estimated savings in cost per MW installed.

For purposes of this conservative analysis, no protective cathodic zinc coating was considered.

OVERVIEW OF STANDARD I-BEAMS

According to the AISC steel construction manual [2], the following W6 sections are standard. In Table 1, t_w represents thickness of the web, t_f thickness of the flange, d is the height of the section and b_f is the flange base width:

I-beam	t_w	t_f	d	b_f
Size	in	in	in	in
6 x 25	0.32	0.455	6.38	6.08
6 x 20	0.26	0.365	6.2	6.02
6 x 15	0.23	0.26	5.99	5.99
6 x 16	0.26	0.405	6.28	4.03
6 x 12	0.23	0.28	6.03	4
6 x 9	0.17	0.215	5.9	3.94
6 x 8.5	0.17	0.195	5.83	3.94

Table 1: Standard I-beam Sections [2]

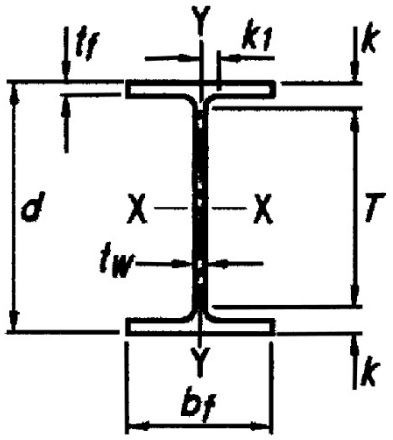

In addition to these standard sizes, Attala Steel provided the dimensions of some less common I-beam sections used by the solar industry, shown in Table 2:

I-beam	t_w	t_f	d	b_f
Size	in	in	in	in
6 x 10.5	0.2	0.25	6.03	4
6 x 7.5	0.144	0.165	5.83	3.9375
6 x 7	0.132	0.165	5.83	3.9375

Table 2: Less Common Steel Sections Used by The Solar Industry

SECTION AND BENDING ANALYSIS

To determine the flexural strength (M_n) or capacity of I-beams, the shape must be evaluated for nominal bending strength, and buckling risk. The nominal bending strength is purely based on the section properties, generally increasing in strength with thickness/width of the flanges and depth of the section. The buckling risk is determined by evaluating the flanges and web for "compactness" and "slenderness". This refers to a ratio of the overall dimensions of the section to the thickness of the section.

If a shape is sufficiently thick, then there is no reduction in capacity due to buckling, and it is determined to be "compact". The point where buckling begins to become a risk factor, the shapes are called "non-compact", and when the shape becomes extremely thin, then it is referred to as "slender". Non-compact and especially slender shapes have the highest likelihood for buckling prior to their bending strength and have special equations that must be used to evaluate their capacities. Typical I-beam shapes do not usually fall into the non-compact and slender categories; however, corrosion actions can cause this to develop over time.

To determine whether a shape falls into a category, they are compared to compactness and slenderness limits. Their size/thickness ratio is compared to a formula based on the yield strength and elasticity of

the material. Generally, as material strength increases, the limits of compactness and slenderness decrease, so higher strength material has more propensity to buckle.

Finally, buckling is also related to the specific loading scenario. The total unsupported length is critical for buckling under bending loads. In the case of the solar foundation, this refers to the distance from the bottom of the pile to the first connection point restricting its movement torsionally.

The following steps describe in detail the process for determining the bending capacity of each of the sections in question, primarily based on the methods in the AISC *Specification for Structural Steel Buildings* [3]. In the calculations, the suggested equations for buckling capacity in the specifications were based on built-up sections rather than hot-rolled sections, so the equations were derived from the hot-rolled ratios to remove discontinuities on the results. The deviations are noted in the methodology below:

1) **Determination of category of flange and web:**

   To determine the category of an I-beam, first the Limiting Width-Thickness Ratios for Compression Elements table was used:

   For flexure in flanges of rolled I-shaped sections and channels, find width Thickness ratio:

   $\lambda = \frac{b_f}{2t_f}$, where b_f is the flange width, in (mm) and t_f is the thickness of flange, in (mm)

   $\lambda_p = \lambda_{pf} = 0.38\sqrt{\frac{E}{F_Y}}$ Compact case limiting value

   $\lambda_r = \lambda_{rf} = 1.0\sqrt{\frac{E}{F_Y}}$ Non-compact case limiting value

   For flexure in webs of doubly symmetric I-shaped sections and channels, find width Thickness ratio: $\frac{h}{t_w}$, where:

   h is the height of the web, in (mm). It can be determined by $h = d - \left(2t_f\right)$, where d is the total height of the I beam, in (mm), and t_w is the web thickness, in (mm).

   $\lambda_p = \lambda_{pw} = 3.76\sqrt{\frac{E}{F_Y}}$ Compact case limiting value

   $\lambda_r = \lambda_{rw} = 5.70\sqrt{\frac{E}{F_Y}}$ Non-compact case limiting value

   where E is the young's Modulus and F_y is the minimum yield stress of steel.

   When λ is less than or equal to λ_p, the section being considered is considered as compact. If λ is less than or equal to λ_r but greater than λ_p then the section is considered as noncompact. If the ratio is greater than λ_r then the section is considered as slender.

   After finding out the category of flange and web, the correct case (2, 3, 4, or 5) below needs to be applied, based on the combination of compactness properties of the section.

2) **Capacity for sections with compact webs and compact flanges:**

   The nominal flexural strength, M_n, shall be the lower value obtained according to the limit states of yielding (plastic moment) and lateral-torsional buckling.

i) Yielding

$M_n = M_p = F_y Z_x$

F_y = specified minimum yield stress of the steel grade being used, Ksi (MPa)

Z_x = plastic section modulus about the x-axis, in^3 (mm^3)

ii) Lateral Torsional Buckling (LTB)

Application of Lateral Torsional Buckling depends on the limiting lengths L_b, L_r and L_p.

L_b = Length between points that are either braced against lateral displacement of compression flange or braced against twist of the cross section, in (mm)

L_p = Limiting laterally unbraced length for the limit state of yielding, in (mm)

L_r = Limiting laterally unbraced length for the limit state of inelastic lateral-torsional buckling, in (mm)

In the current case L_b is taken as 72 in (6 ft), which is the length from top to the point of fixity.

The limiting lengths L_p and L_r can be found using:

$$L_p = 1.76\, r_y \sqrt{\frac{E}{F_y}} \quad \text{and} \quad L_r = 1.95\, r_{ts} \frac{E}{0.7\, F_Y} \sqrt{\frac{Jc}{S_x h_o} + \sqrt{\left(\frac{Jc}{S_x h_o}\right)^2 + 6.76\left(\frac{0.7\, F_y}{E}\right)^2}}$$

Where $r_{ts} = \frac{\sqrt{I_y C_w}}{S_x}$

for a doubly symmetric I-shape: c = 1

h_o = distance between the flange centroids, in (mm)

E = modulus of elasticity of steel = 29,000 Ksi (200,000 MPa)

J = torsional constant, in^4 (mm^4)

S_x = elastic section modulus taken about the x-axis, in^3 (mm^3)

C_w = warping constant, in^6 (mm^6). For doubly symmetric I-shapes with rectangular flanges,

$$C_w = \frac{I_y h_o^2}{4}$$

The lateral-torsional buckling modification factor, C_b, is for nonuniform moment diagrams when both ends of the unsupported segment are braced. This can be taken as 1.67, assuming zero moment at one end, however other load cases including moments would result in different values.

Lateral Torsional Buckling cases:

a) When $L_b \leq L_p$, the limit state of lateral torsional buckling does not apply

b) When $L_p < L_b \leq L_r$

$$M_n = C_b \left[M_p - \left(M_p - 0.7 F_y S_x\right)\left(\frac{L_b - L_p}{L_r - L_p}\right)\right] \leq M_p$$

c) When $L_b > L_r$

$$M_n = F_{cr}\, S_x \leq\ M_p$$

Where,

$$F_{cr} = \frac{C_b \pi^2 E}{\left(\frac{L_b}{r_{ts}}\right)^2} \sqrt{1 + 0.078 \frac{Jc}{S_x h_o} \left(\frac{L_b}{r_{ts}}\right)^2}$$

3) Capacity for sections with compact webs and non-compact or slender flanges:

The nominal Flexural strength, M_n, shall be the lower value obtained according to the limit states of lateral-torsional buckling and compression flange local buckling.

i) Lateral Torsional Buckling (LTB) is evaluated same as above.

ii) Compression Flange Local Buckling

a) For sections with noncompact flanges

$$M_n = \left[M_p - \left(M_p - 0.7 F_y S_x\right)\left(\frac{\lambda - \lambda_{pf}}{\lambda_{rf} - \lambda_{pf}}\right)\right]$$

b) For sections with slender flanges, the equation used in the AISC manual was derived from built-up section slenderness limits and resulted in discontinuities in the properties of the I-beams as they corroded. Applying the assumption that at the slenderness limit $\lambda = \sqrt{E/F_y}$, the following relationship was derived:

$$M_n = \frac{0.7\ E\ S_x}{\lambda^2}$$

4) Capacity for sections with non-compact webs:

The nominal flexural strength, M_n, shall be the lowest value obtained according to the limit states of compression flange yielding, lateral-torsional buckling, compression flange local buckling and tension flange yielding.

i) Compression Flange Yielding

$$M_n = R_{pc} M_y = R_{pc} F_y S_x$$

ii) Lateral-Torsional Buckling

a) When $L_b \leq L_p$, the limit state of lateral-torsional buckling does not apply.

b) When $L_p \leq L_b \leq L_r$

$$M_n = C_b \left[R_{pc}\, M_y - \left(R_{pc} M_y - F_L S_x\right)\left(\frac{L_b - L_p}{L_r - L_p}\right)\right] \leq R_{pc}\, M_y$$

c) When $L_b > L_r$

$$M_n = F_{cr} S_x \leq R_{pc} M_y$$

$$M_y = F_y S_x$$

$$F_{cr} = \frac{C_b \pi^2 E}{\left(\frac{L_b}{r_t}\right)^2} \sqrt{1 + 0.078 \frac{J}{S_x h_o} \left(\frac{L_b}{r_t}\right)^2}$$

The stress, F_L, is determined: $F_L = 0.7F_y$

The limiting laterally unbraced length for the limit state of yielding, L_p, is

$$L_p = 1.1 r_t \sqrt{\frac{E}{F_y}}$$

The limiting laterally unbraced length for the limit state of inelastic lateral-torsional buckling, L_r, is the same as the compact case.

d) For $\frac{h_c}{t_w} \leq \lambda_{pw}$

$$R_p = \frac{M_p}{M_y}$$

e) For $\frac{h_c}{t_w} > \lambda_{pw}$

$$R_{pc} = \left[\frac{M_p}{M_y} - \left(\frac{M_p}{M_y} - 1\right)\left(\frac{\lambda - \lambda_{pw}}{\lambda_{rw} - \lambda_{pw}}\right)\right] \leq \frac{M_p}{M_y}$$

Where,

$M_p = Z_x F_y \leq 1.6 S_x F_y$

The effective radius of gyration for lateral-torsional buckling, r_t for I-shapes with a rectangular compression flange is determined by:

$$r_t = \frac{b_{fc}}{\sqrt{12\left(\frac{h_o}{d} + \frac{1}{6}a_w\right)}}, \qquad a_w = \frac{h_c t_w}{b_f t_f}$$

iii) Compression Flange Local Buckling

a) For sections with compact flanges, the *limit state* of *local buckling* does not apply.
b) For sections with non-compact flanges

$$M_n = \left[R_{pc}\, M_y - \left(R_{pc} M_y - F_L S_x\right)\left(\frac{\lambda - \lambda_{pf}}{\lambda_{rf} - \lambda_{pf}}\right)\right]$$

c) For sections with slender flanges, again the equation derived from the hot-rolled slenderness limits was used in place of the AISC equation:

$$M_n = \frac{0.7\, E\, S_x}{\lambda^2}$$

5) Capacity for sections with slender webs:

The nominal flexural strength, M_n, shall be the lowest value obtained according to the limit states of compression flange yielding, lateral-torsional buckling, compression flange local buckling and tension flange yielding.

i) Compression Flange Yielding

$$M_n = R_{pg} F_y S_{xc}$$

ii) Lateral-Torsional Buckling

$$M_n = R_{pg} F_{cr} S_{xc}$$

a) When $L_b \leq L_p$, the limit state of lateral-torsional buckling does not apply.

b) When $L_p \leq L_b \leq L_r$

$$F_{cr} = C_b \left[F_y - (0.3F_y) \left(\frac{L_b - L_p}{L_r - L_p} \right) \right] \leq F_y$$

c) When $L_b > L_r$

$$F_{cr} = \frac{C_b \pi^2 E}{\left(\frac{L_b}{r_t}\right)^2} \leq F_y \qquad L_r = \pi r_t \sqrt{\frac{E}{0.7F_y}}$$

R_{pg} is the bending strength reduction factor:

$$R_{pg} = 1 - \frac{a_w}{1200 + 300a_w} \left(\frac{h_c}{t_w} - 5.7 \sqrt{\frac{E}{F_y}} \leq 1.0 \right)$$

iii) Compression Flange Local Buckling

$$M_n = R_{pg} F_{cr} S_{xc}$$

a) For sections with compact flanges, the limit state of compression flange local buckling does not apply.

b) For sections with noncompact flanges

$$F_{cr} = \left[F_y - (0.3F_y) \left(\frac{\lambda - \lambda_{pf}}{\lambda_{rf} - \lambda_{pf}} \right) \right]$$

c) For sections with slender flange sections, the AISC proposed equation again resulted in discontinuities due to the equation being based on built-up sections rather than rolled sections, so the following equation was derived for use in this study:

$$F_{cr} = \frac{0.7\ E}{\left(\frac{b_f}{2t_f}\right)^2}$$

According to this methodology, all the combinations of section properties, material strength, and corrosion potential were analyzed. For a basis of comparison, Table 3 shows calculated values for flexural strength, pre-corrosion for 50 ksi material:

Typical I-beam Weight and Flexural Strength (50 ksi)		
I-beam	**Weight (lb/ft)**	**M_n (k-in)**
6 x 25	24.86	946.70
6 x 20	19.88	746.57
6 x 16	16.03	584.85
6 x 15	14.96	509.81
6 x 12	11.99	416.82
6 x 10.5	10.57	365.45
6 x 9	9.01	312.62
6 x 8.5	8.45	280.94
6 x 7.5	7.12	221.85
6 x 7	6.89	217.78

Table 3: 50 ksi Weights and Bending Strength

CORROSION RATES AND ASSUMPTIONS

To simplify this analysis, the requirements in Table 4 are proposed by the American Association of State Highway and Transportation Officials (AASHTO) [4] for mildly corrosive soils. The more aggressive rates, also shown in Table 4, are chosen as multiples of the corrosion rates to simulate higher corrosivity environments.

Assumed Corrosion Rates			
	AASHTO (1X)	**2X**	**3X**
Carbon Steel Rate	**0.47 mils/yr (12um/yr)**	**0.94 mils/yr (24 um/yr)**	**1.41 mils/yr (36 um/yr)**

Table 4: AASHTO Corrosion Rates and Multiplied Values [4]

Applicability of these corrosion rates depends on many factors, including whether the soil has been disturbed, its makeup, pH, resistivity, and moisture content, as well as other factors. The USDA has created the map in Figure 1 to show the relative risk of corrosion in steel piles in the U.S. [5][1]

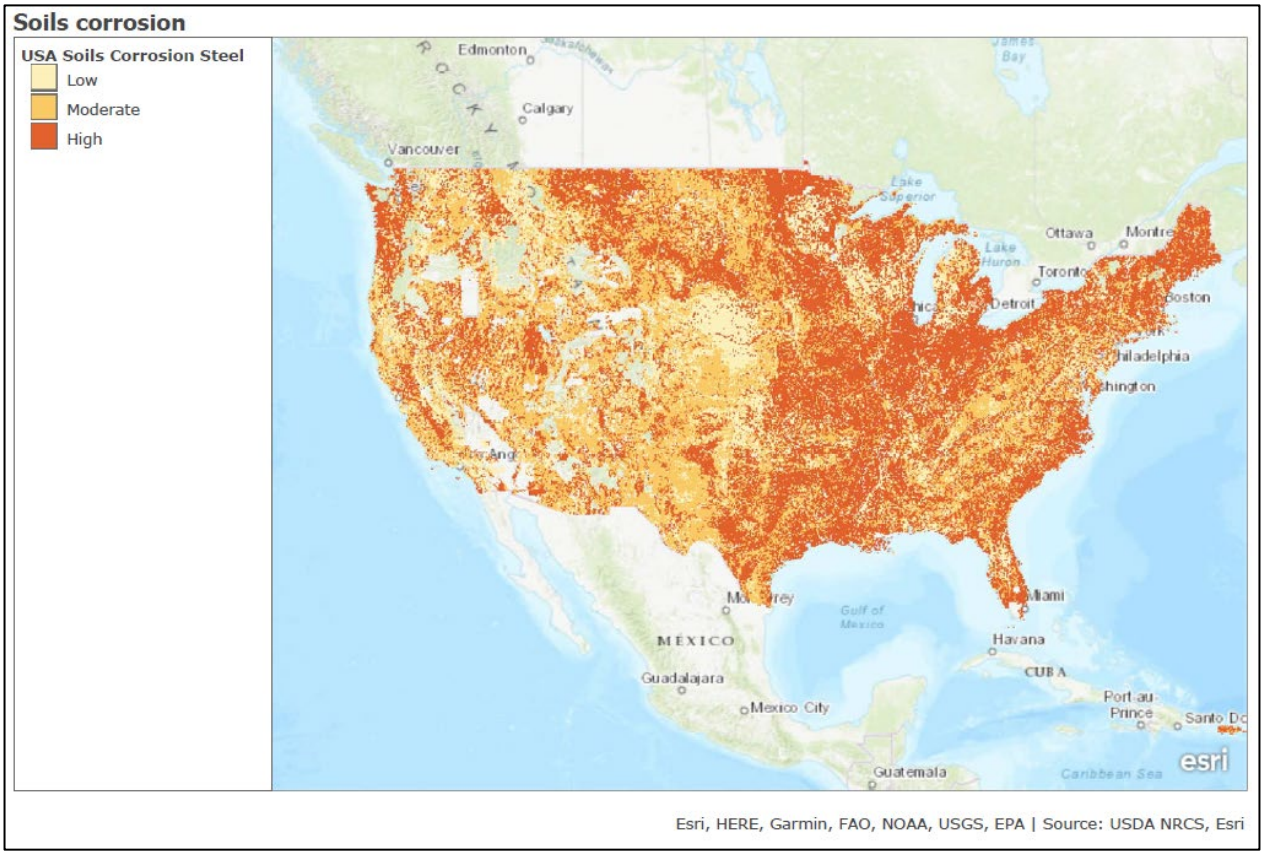

Figure 1: Corrosion risk for steel in the USA. [5]

[1] This figure includes intellectual property of Esri and its licensors and are used under license. Copyright ©2018 Esri and its licensors. All rights reserved.

As previously noted, an ASTM A123 [1] zinc coating was conservatively neglected for the purposes of this study. It should be noted that in many corrosion areas, hot-dip galvanizing can prevent much or all the steel corrosion. The charts in Figure 2, from the American Galvanizer's Association [6], shows the time to replace steel components due to soil corrosion in various soil conditions. According to these results, in many applications galvanized steel articles may last the entire lifespan without service. For the purposes of this study, highly corrosive soils, such as shown in Figure 2-Chart 2 for high chlorides and moisture are being considered. [6] These results are based on the research of Corrpro, in their study "Soil Side Durability of Corrugated Steel Pipe", in which 122 sites across the United States were evaluated. [7] The charts created by the AGA show the entire range of moisture and chloride contents, as well as pH values found in the study.

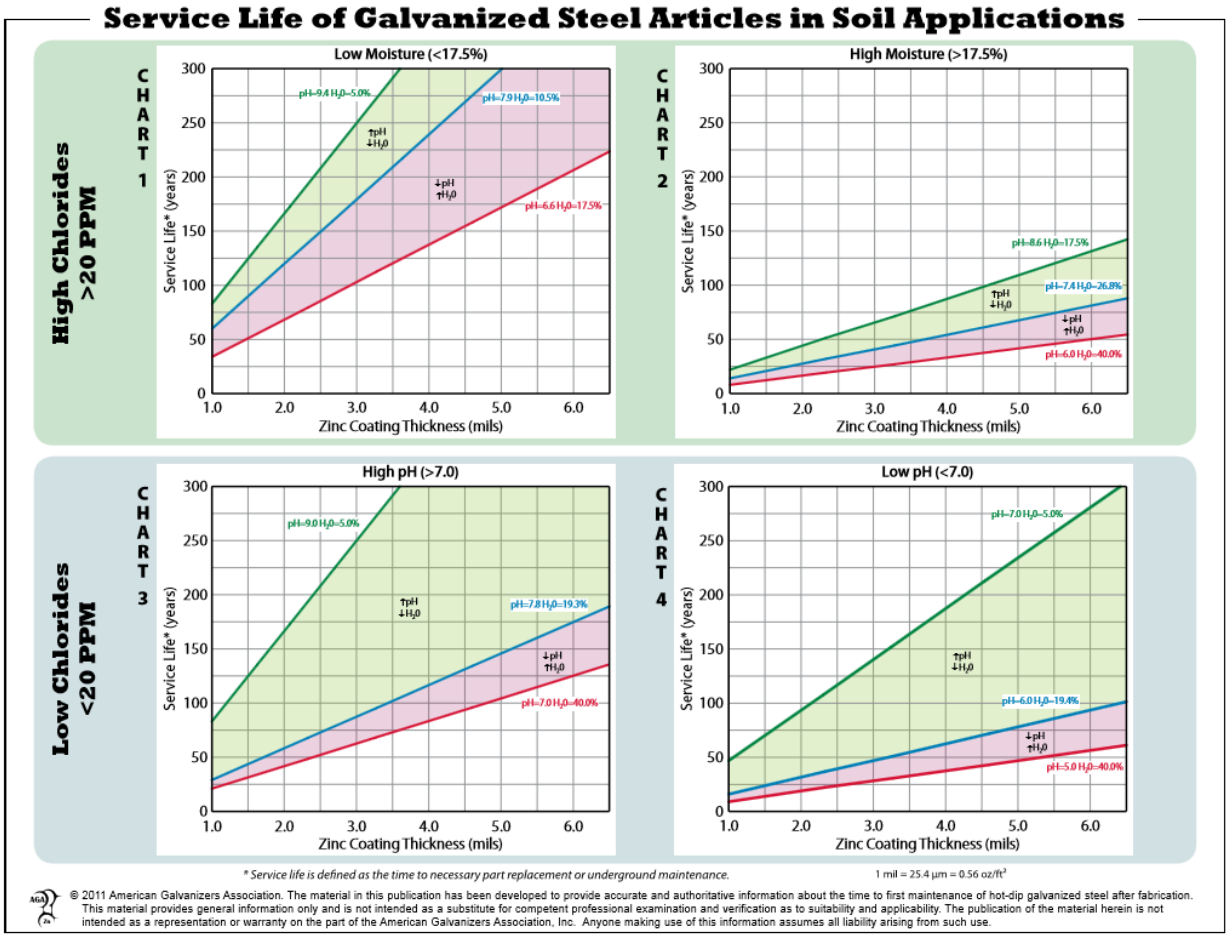

Figure 2: AGA Estimated Service Life for Galvanized Steel in Soils [6] ©American Galvanizers Association – Used with permission

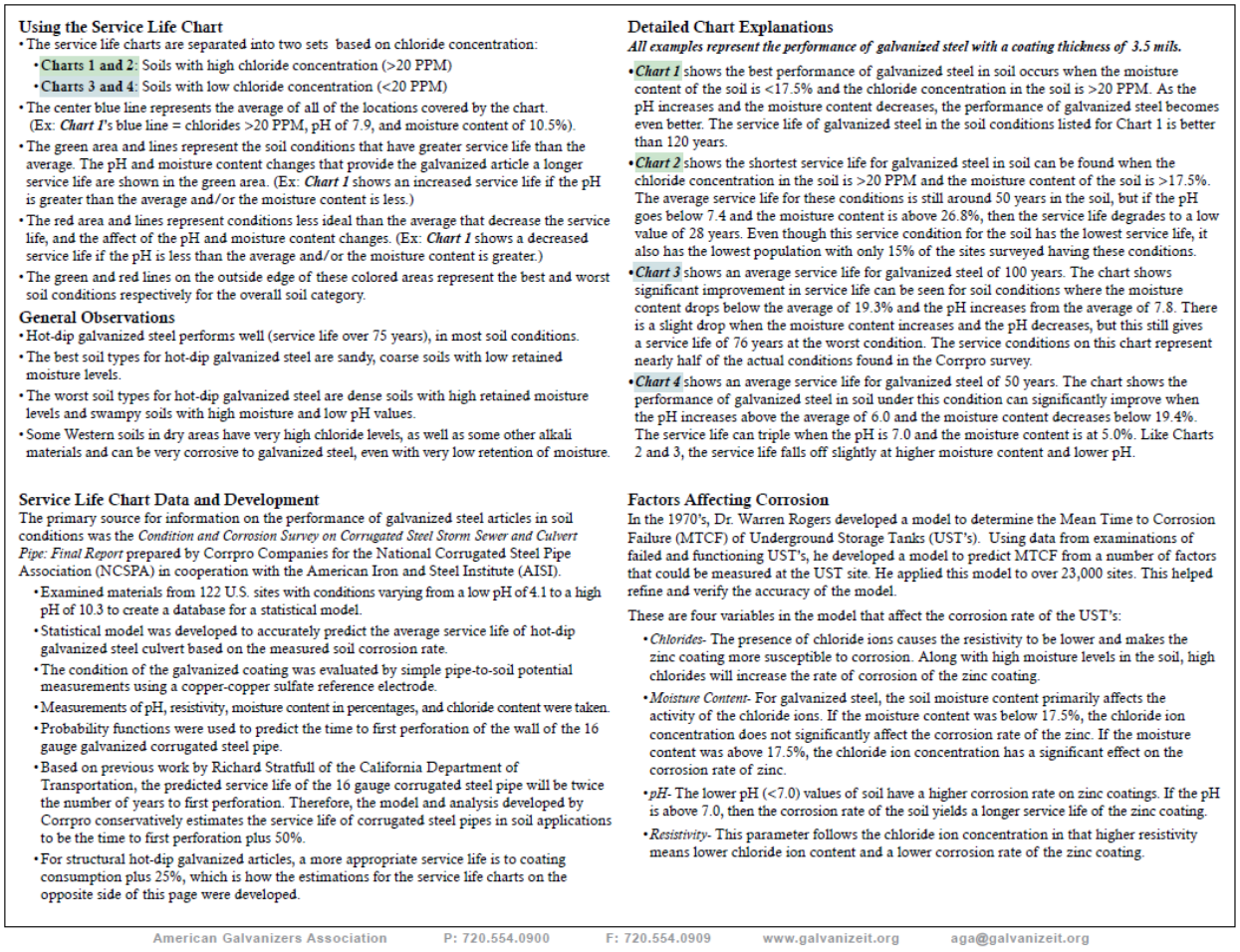

Using the Service Life Chart

- The service life charts are separated into two sets based on chloride concentration:
  - **Charts 1 and 2**: Soils with high chloride concentration (>20 PPM)
  - **Charts 3 and 4**: Soils with low chloride concentration (<20 PPM)
- The center blue line represents the average of all of the locations covered by the chart. (Ex: ***Chart 1***'s blue line = chlorides >20 PPM, pH of 7.9, and moisture content of 10.5%).
- The green area and lines represent the soil conditions that have greater service life than the average. The pH and moisture content changes that provide the galvanized article a longer service life are shown in the green area. (Ex: ***Chart 1*** shows an increased service life if the pH is greater than the average and/or the moisture content is less.)
- The red area and lines represent conditions less ideal than the average that decrease the service life, and the affect of the pH and moisture content changes. (Ex: ***Chart 1*** shows a decreased service life if the pH is less than the average and/or the moisture content is greater.)
- The green and red lines on the outside edge of these colored areas represent the best and worst soil conditions respectively for the overall soil category.

General Observations

- Hot-dip galvanized steel performs well (service life over 75 years), in most soil conditions.
- The best soil types for hot-dip galvanized steel are sandy, coarse soils with low retained moisture levels.
- The worst soil types for hot-dip galvanized steel are dense soils with high retained moisture levels and swampy soils with high moisture and low pH values.
- Some Western soils in dry areas have very high chloride levels, as well as some other alkali materials and can be very corrosive to galvanized steel, even with very low retention of moisture.

Service Life Chart Data and Development

The primary source for information on the performance of galvanized steel articles in soil conditions was the *Condition and Corrosion Survey on Corrugated Steel Storm Sewer and Culvert Pipe: Final Report* prepared by Corrpro Companies for the National Corrugated Steel Pipe Association (NCSPA) in cooperation with the American Iron and Steel Institute (AISI).

- Examined materials from 122 U.S. sites with conditions varying from a low pH of 4.1 to a high pH of 10.3 to create a database for a statistical model.
- Statistical model was developed to accurately predict the average service life of hot-dip galvanized steel culvert based on the measured soil corrosion rate.
- The condition of the galvanized coating was evaluated by simple pipe-to-soil potential measurements using a copper-copper sulfate reference electrode.
- Measurements of pH, resistivity, moisture content in percentages, and chloride content were taken.
- Probability functions were used to predict the time to first perforation of the wall of the 16 gauge galvanized corrugated steel pipe.
- Based on previous work by Richard Stratfull of the California Department of Transportation, the predicted service life of the 16 gauge corrugated steel pipe will be twice the number of years to first perforation. Therefore, the model and analysis developed by Corrpro conservatively estimates the service life of corrugated steel pipes in soil applications to be the time to first perforation plus 50%.
- For structural hot-dip galvanized articles, a more appropriate service life is to coating consumption plus 25%, which is how the estimations for the service life charts on the opposite side of this page were developed.

Detailed Chart Explanations

All examples represent the performance of galvanized steel with a coating thickness of 3.5 mils.

- ***Chart 1*** shows the best performance of galvanized steel in soil occurs when the moisture content of the soil is <17.5% and the chloride concentration in the soil is >20 PPM. As the pH increases and the moisture content decreases, the performance of galvanized steel becomes even better. The service life of galvanized steel in the soil conditions listed for Chart 1 is better than 120 years.
- ***Chart 2*** shows the shortest service life for galvanized steel in soil can be found when the chloride concentration in the soil is >20 PPM and the moisture content of the soil is >17.5%. The average service life for these conditions is still around 50 years in the soil, but if the pH goes below 7.4 and the moisture content is above 26.8%, then the service life degrades to a low value of 28 years. Even though this service condition for the soil has the lowest service life, it also has the lowest population with only 15% of the sites surveyed having these conditions.
- ***Chart 3*** shows an average service life for galvanized steel of 100 years. The chart shows significant improvement in service life can be seen for soil conditions where the moisture content drops below the average of 19.3% and the pH increases from the average of 7.8. There is a slight drop when the moisture content increases and the pH decreases, but this still gives a service life of 76 years at the worst condition. The service conditions on this chart represent nearly half of the actual conditions found in the Corrpro survey.
- ***Chart 4*** shows an average service life for galvanized steel of 50 years. The chart shows the performance of galvanized steel in soil under this condition can significantly improve when the pH increases above the average of 6.0 and the moisture content decreases below 19.4%. The service life can triple when the pH is 7.0 and the moisture content is at 5.0%. Like Charts 2 and 3, the service life falls off slightly at higher moisture content and lower pH.

Factors Affecting Corrosion

In the 1970's, Dr. Warren Rogers developed a model to determine the Mean Time to Corrosion Failure (MTCF) of Underground Storage Tanks (UST's). Using data from examinations of failed and functioning UST's, he developed a model to predict MTCF from a number of factors that could be measured at the UST site. He applied this model to over 23,000 sites. This helped refine and verify the accuracy of the model.

These are four variables in the model that affect the corrosion rate of the UST's:

- *Chlorides*- The presence of chloride ions causes the resistivity to be lower and makes the zinc coating more susceptible to corrosion. Along with high moisture levels in the soil, high chlorides will increase the rate of corrosion of the zinc coating.
- *Moisture Content*- For galvanized steel, the soil moisture content primarily affects the activity of the chloride ions. If the moisture content was below 17.5%, the chloride ion concentration does not significantly affect the corrosion rate of the zinc. If the moisture content was above 17.5%, the chloride ion concentration has a significant effect on the corrosion rate of zinc.
- *pH*- The lower pH (<7.0) values of soil have a higher corrosion rate on zinc coatings. If the pH is above 7.0, then the corrosion rate of the soil yields a longer service life of the zinc coating.
- *Resistivity*- This parameter follows the chloride ion concentration in that higher resistivity means lower chloride ion content and a lower corrosion rate of the zinc coating.

American Galvanizers Association P: 720.554.0900 F: 720.554.0909 www.galvanizeit.org aga@galvanizeit.org

Figure 3: Usage notes for AGA Estimated Service Life for Galvanized Steel in Soils [6] ©American Galvanizers Association – Used with permission

To help with interpreting the results of these charts for the purposes of steel foundation design, there is a paper also published by the AGA, "Predicting Galvanized Steel's Service Life in Soil Applications". [8] According to this paper, the service life shown in the charts above is defined as the "time to complete consumption of the galvanized coating plus an extra 25% of that time." Therefore, to predict the time to completely consume the zinc on a pile using the charts above, the service life from the chart must be divided by 1.25. For example, using the most conservative example with high moisture at 40%, a pH of 6.0, and a zinc thickness of 3.0 mils, the expected service life is 25 years, and the time to complete zinc depletion would be 25/1.25 = 20 years.

RESULTS AND DISCUSSION

An example of the initial bending capacities of each of the sections can be found in Table 5 below, along with the resulting reductions in moment capacity (M_n) and weight after corrosion occurs.

AASHTO corrosion for 30 years, 50 KSI material					
I-beam	**Weight (lb/ft) before**	**M_n before (k-in)**	**M_n after (k-in)**	**Weight (lb/ft) after**	**Equiv. I-beam after**
6 x 25	24.86	946.7	924.5	24.25	6 x 24.5
6 x 20	19.88	746.6	725.0	19.27	6 x 19.5
6 x 16	16.03	584.8	568.9	15.56	6 x 15.5
6 x 15	14.96	509.8	484.8	14.37	6 x 14.5
6 x 12	11.99	416.8	401.5	11.52	6 x 11.5
6 x 10.5	10.57	365.5	344.2	9.94	6 x 10
6 x 9	9.01	312.6	288.3	8.39	6 x 8.5
6 x 8.5	8.45	280.9	256.9	7.84	6 x 8
6 x 7.5	7.12	221.8	193.1	6.39	6 x 6.5
6 x 7	6.89	217.8	189.2	6.16	6 x 6

Table 5: 50 ksi reduction in weight and strength, standard AASHTO corrosion

The same process was performed for each of the cases (50 ksi ,65 ksi, and 80 ksi), and (1X, 2X, and 3X AASHTO corrosion rates). Note that some of these shapes begin as compact but become more non-compact or slender after the corrosion effects are applied, particularly in higher strength materials. This results in a non-linear reduction in strength. This is particularly true in higher corrosion and higher strength materials.

In Figure 4, the weight reductions after 30 years of continuous corrosion are shown at the three different rates.

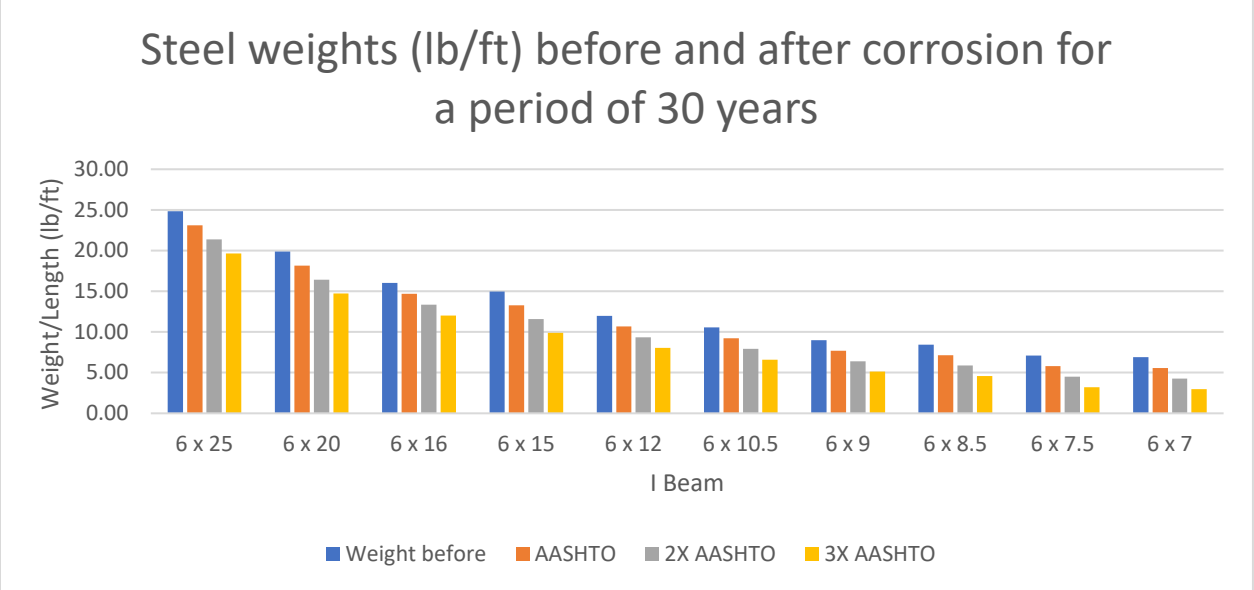

Figure 4: Steel Weight Reductions over 30 years in Various Corrosive Conditions

The capacities at each corrosion level was evaluated at various strength materials, and the resultant reductions in capacities are shown in Figures 5-7.

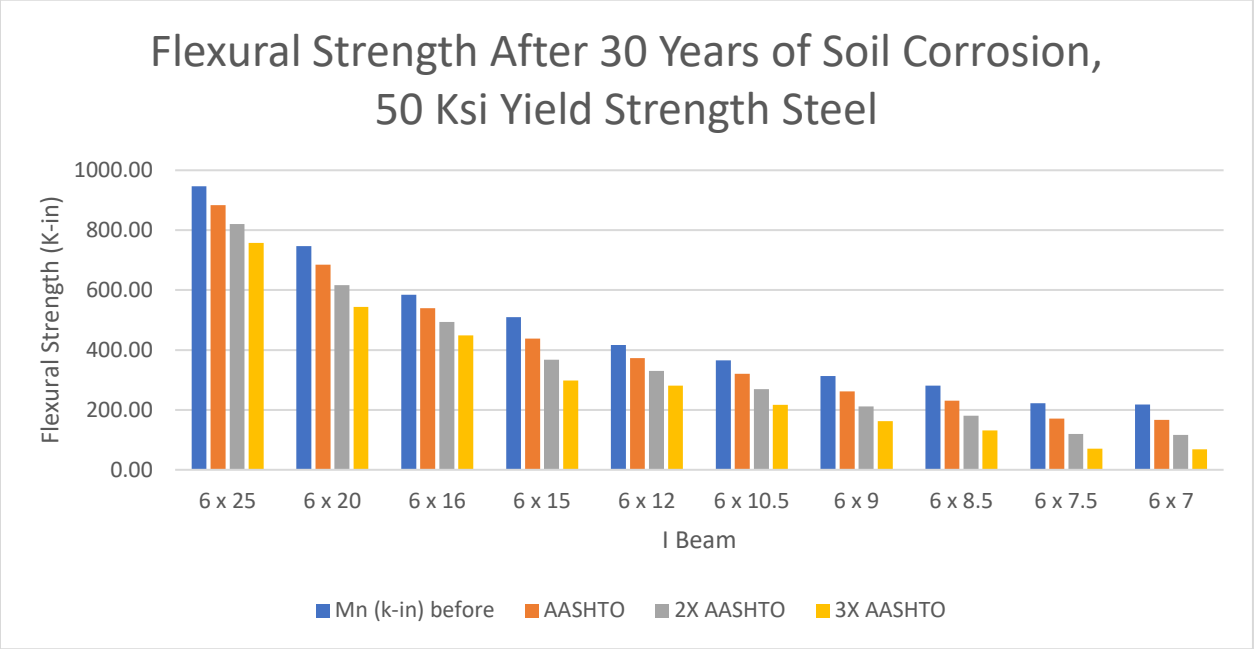

Figure 5: 50 ksi Yield Strength Reductions

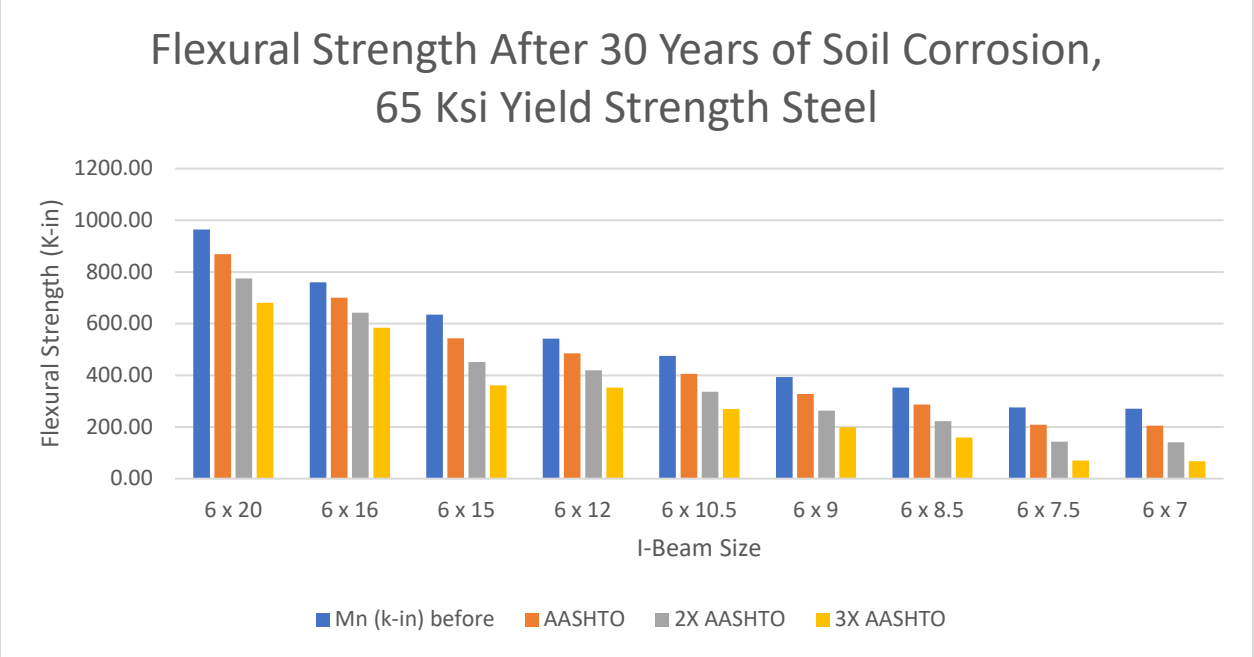

Figure 6: 65 ksi Yield Strength Reductions

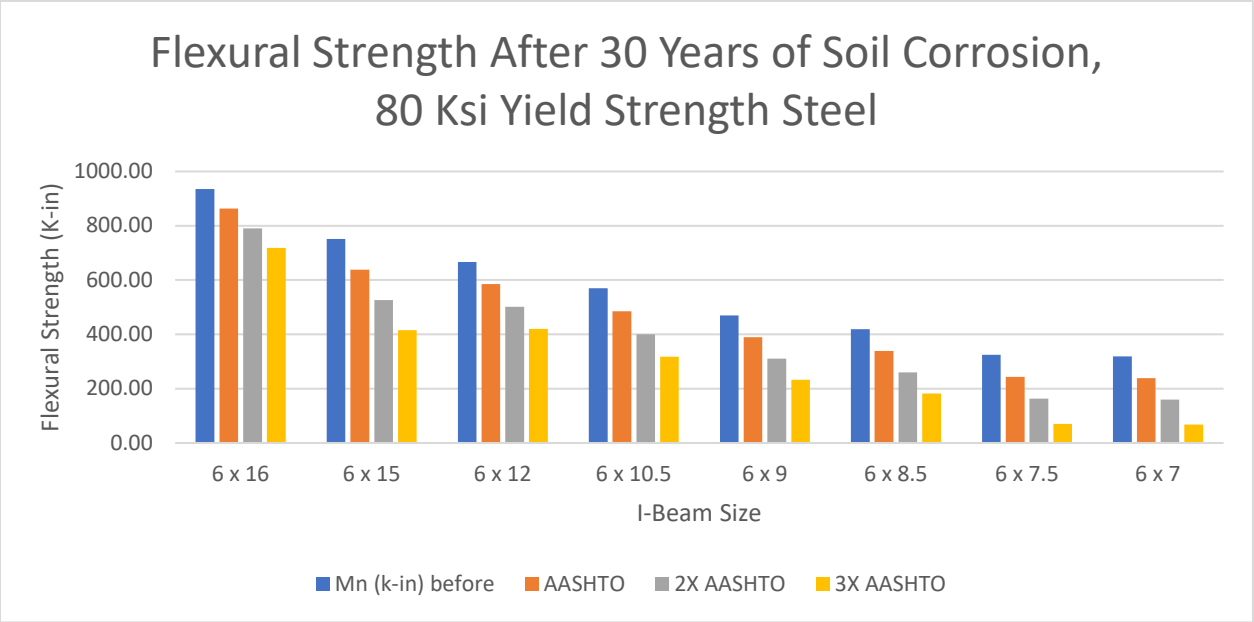

Figure 7: 80 ksi Yield Strength Reductions

In many cases, at the higher corrosion rates, the smaller size beams are reduced to half of their original capacity or become so slender that they cannot be used at all. However, the higher strength materials retain capacities far greater than the lower strength I-beams. They can therefore be used in higher corrosion applications in lighter weights than the equivalent 50 ksi materials. In Tables 6-8 below, equivalent strength sizes are shown based on the three corrosion cases:

AASHTO (Mild) Pier Size vs Post-Corrosion Strength					
80 KSI equivalent		**65 KSI equivalent**		**50 KSI**	
Size	**M_n (k-in)**	**Size**	**M_n (k-in)**	**Size**	**M_n (k-in)**
6 x 16	862.9	6 x 20	869.0	6 x 25	883.4
6 x 15	638.3	6 x 16	701.1	6 x 20	685.2
6 x 12	584.9	6 x 15	542.8	6 x 16	539.3
6 x 10.5	485.0	6 x 12	485.2	6 x 15	438.5
6 x 9	389.6	6 x 10.5	405.8	6 x 12	373.3
6 x 8.5	339.0	6 x 9	327.6	6 x 10.5	320.7
6 x 7.5	243.4	6 x 8.5	286.8	6 x 9	261.6
6 x 7	238.5	6 x 7.5	209.0	6 x 8.5	230.4
		6 x 7	204.7	6 x 7.5	170.5

Table 6: Equivalent Sections for Mild Corrosion

2X AASHTO (Medium) Pier Size vs Post-Corrosion Strength					
80 KSI equivalent		**65 KSI equivalent**		**50 KSI**	
Size	**M_n (k-in)**	**Size**	**M_n (k-in)**	**Size**	**M_n (k-in)**
6 x 16	790.5	6 x 20	774.5	6 x 25	820.4
6 x 16	790.5	6 x 16	642.3	6 x 20	616.2
6 x 12	501.9	6 x 15	451.5	6 x 16	494.1
6 x 10.5	400.7	6 x 12	419.4	6 x 15	367.9
6 x 9	310.2	6 x 10.5	336.9	6 x 12	330.0
6 x 8.5	260.1	6 x 9	262.7	6 x 10.5	269.0
6 x 8.5	260.1	6 x 8.5	222.4	6 x 9	211.4
6 x 7.5	163.6	6 x 8.5	222.4	6 x 8.5	180.6
		6 x 7	140.3	6 x 7.5	120.0

Table 7: Equivalent Sections for Medium Corrosion

3X AASHTO (High) Pier Size vs Post-Corrosion Strength					
80 KSI equivalent		**65 KSI equivalent**		**50 KSI**	
Size	**M_n (k-in)**	**Size**	**M_n (k-in)**	**Size**	**M_n (k-in)**
6 x 16	718.6	6 x 20	681.1	6 x 25	757.7
6 x 16	718.6	6 x 16	583.9	6 x 20	543.8
6 x 12	420.1	6 x 16	583.9	6 x 16	449.1
6 x 10.5	317.8	6 x 12	352.5	6 x 15	298.0
6 x 10.5	317.8	6 x 10.5	269.2	6 x 12	280.9
6 x 9	232.4	6 x 9	199.1	6 x 10.5	216.5
6 x 8.5	182.7	6 x 8.5	159.1	6 x 9	162.1
		6 x 8.5	159.1	6 x 8.5	131.6
		6 x 7	68.1	6 x 7.5	70.6

Table 8: Equivalent Sections for High Corrosion

Comparing the flexural strength of the sections before and after corrosion, as the sections get thinner, and material loss percentage due to corrosion more aggressive, the strength increase declines, but is still substantial even at the lowest weight beam size.

One interesting result of the analysis was that the W6x15 size beams seems to be an outlier on Figure 8. This is due to the larger flange width (~6") of the W6x15 falling in the same size family as the W6x20 and W6x25 vs. the more typical 4" width of W6 sizes. This larger flange size both causes greater surface area therefore more material losses due to corrosion, and

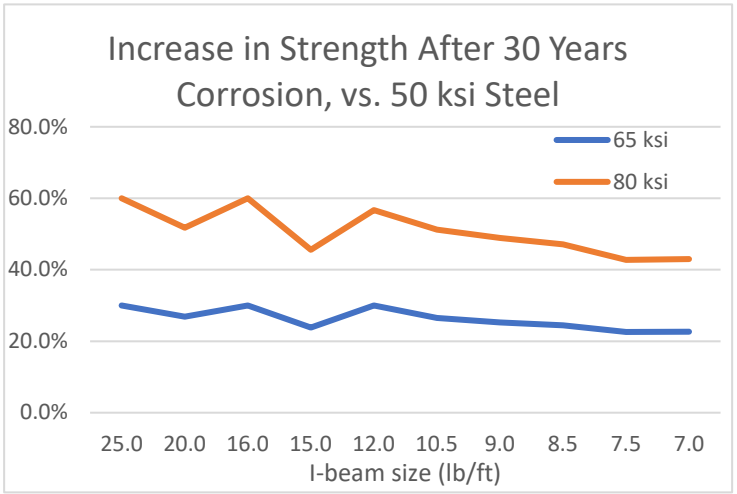

Figure 8: Strength Comparison in Higher Strength Steels After 30 Years Corrosion

greater capacity reductions due to buckling. It is commonly assumed that increasing I-beam weight has a proportional increase in capacity, but this is not necessarily true when changing size families.

The higher yield materials are then evaluated for equivalent post-corrosion strength for comparison to the 50 ksi sections. To show the cost reduction for higher strength options, prices were estimated using input from Attala Steel, and historical hot-rolled steel market values. As actual steel and rare metal prices change constantly, an approximation for material costs was used to estimate potential savings. The following pricing per unit weight was used for each grade of steel: 50 ksi-$0.650/lb, 65 ksi-$0.675/lb, and 80 ksi-$0.700/lb. These are theoretical prices assuming standard in-stock material with normal scrap rates and established supply chain. For the solar site cost analysis, it is assumed that each foundation is 10 feet in length and supports 2880W (360W x 8) worth of solar panels.

This analysis was applied to each post, for each corrosion situation for the higher strength posts. Interestingly, the reduction in size, and therefore cost, holds almost constant with respect to corrosion rates, and so the decrease in cost shown below is based on an average of the 3 cases above.

In situations where specified 50 ksi posts are heavier sizes (>9 lb/ft), there is a significant cost savings potential, ranging from $2,000-$10,000/MW, depending on the sizes and quantities of the foundations required. The general trend in cost savings aligns with the size of foundation, with more potential as the posts get heavier.

Transportation costs are a significant factor that will also be affected by using higher strength materials to reduce section size. Since the cost to transport one pound of steel to site is the same regardless of grade, whatever the percentage reduction of section size would be the additional percentage savings in freight costs. Thus, if grade 80 steel was utilized and that resulted in a 15% reduction in section size, then the freight costs would also be reduced by approximately 15%.

CONCLUSIONS

Many different parameters affect the costs and utility of foundations, but the increased costs for the higher strength materials are more than justified by the increased performance. Besides the apparent benefits to strength and cost-reduction opportunities, using less material is beneficial environmentally, due to reductions in transportation and processing required to produce the foundations.

In addition to the material cost reduction, “soft costs” can be reduced as well, such as stocking, handling, storage, and installation. The higher strength materials will be more resilient against damage during pile-driving and other operations, and transportation costs onsite will be reduced since more material can be moved at one time.

Various combinations of size and material may be custom, requiring additional lead time and stocking fees if specified on a project. Enough quantity in a specific configuration should amortize the costs enough to overcome these issues in the long term, however.

Certain parameters could change the results of this report. Closing the cost gap between the steel materials would improve the economics for all sites, and vice versa. The design assumptions for the pile sizes are small compared to many solar foundation designs. In areas with frost heave or expansive clays, for example, pile lengths of over 20 feet long may be required. If long piles are required, the savings will scale proportionally to the length.

Since there is opportunity to reduce cost while also improving resiliency of the piles, this approach can be safely tested by choosing pile sizes that decrease cost and increase capacity. There are clear paths for further optimization of shapes and sizes in conjunction to the material optimization as well, to further improve the efficiency of the shapes and enhance cost reduction opportunities.

In conclusion, this higher strength foundation material is a very promising path forward to reduce solar costs for projects that require W6 wide flange hot-rolled I-beams as foundation supports.

Works Cited

[1] ASTM A123 – *Zinc (Hot-Dip Galvanized) Coatings on Iron and Steel Products*, ASTM A 123/A 123M -02, December 2002.

[2] American Institute of Steel Construction, *Steel Construction Manual, 15th ed.*, USA, 2018.

[3] American Institute of Steel Construction, *Specification for Structural Steel Buildings*, USA, 2016

[4] Victor Elias, P.E., Kenneth L. Fishman, Ph.D., P.E., Barry R. Christopher, Ph.D., P.E. and Ryan R. Berg, P.E., "Corrosion/Degradation of Soil Reinforcements for Mechanically Stabilized Earth Walls and Reinforced Soil Slopes," Ryan R. Berg & Associates, Inc., National Highway Institute Federal Highway Administration, Report No. FHWA-NHI-09-087, November 2009.

[5] USDA Natural Resources Conservation Service, "USA Soils Corrosion Steel," Esri. [Online]. Available: https://landscape11.arcgis.com/arcgis/rest/services/USA_Soils_Corrosion_Steel/ImageServer. [Accessed September 18, 2018].

[6] American Galvanizers Association, "Service Life of Galvanized Steel Articles in Soil Applications," AGA. [Online]. Available: https://galvanizeit.org/uploads/publications/Galvanized_Steel_Performance_in_Soil.pdf. [Accessed October 9, 2018]

[7] Corrpro Companies, Inc., James B. Bushman, P.E., Corwin L. Tracy, P.E., Warren F. Rogers, Ph.D., Julie Gaeckle, "Soil Side Durability of Corrugated Steel Pipe," Prepared for the National Corrugated Steel Pipe Association, The American Iron and Steel Insitute, March 1991.

[8] Daniel Barlow, Alana Hochstein, and Thomas Langill, PhD, "Predicting Galvanized Steel's Service Life in Soil Applications," American Galvanizers Association, August 2015.